Holographic warm inflation

Abolhassan Mohammadi*

Department of Physics, Faculty of Science, University of Kurdistan, Pasdaran Street, P.O. Box 66177-15175 Sanandaj, Iran

(Received 23 September 2021; accepted 23 November 2021; published 17 December 2021)

The increasing interest in studying the role of holographic dark energy in the evolution of the very early Universe motivates us to study it for the scenario of warm inflation. Because of this scenario, the holographic dark energy, which now drives inflation, has an interaction with the radiation. The case of interacting dark energy also has received increasing interest in studying the late time cosmology. The infrared cutoff is taken as the Hubble length, and all corrections are assumed to be exhibited by the parameter c, which appears in the holographic dark energy. By comparing the predictions of the model with observational data, the free constants of the model could be determined. Then, by using these values of the constants, the energy density of inflation is estimated. Next, we consider the validity of the fundamental assumptions of the warm inflation, e.g., $T/H > 1$, which is necessary to be held during inflation, for the obtained values of the constant. Gathering all outcomes, the model could be counted as a suitable candidate for warm inflation.

DOI: 10.1103/PhysRevD.104.123538

I. INTRODUCTION

Since the first proposal of inflation [1,2] and its preliminary modifications [3–5], many different models of inflation in different frames have been introduced [6–39]. So far, the scenario of inflation has received wide acceptance from cosmologists, and it has been supported strongly by the observational data [40–42].

Based on the scenario, it is assumed that the scalar field is the dominant component that drives inflation. It is called inflaton. The energy density of the scalar field includes a kinetic term and a potential one. Since the scalar field varies slowly, the potential term dominates over the kinetic term. Then, the equation of the state is about $\omega \simeq -1$, and a quasi–de Sitter expansion occurs [43–51]. Because of this extreme expansion, all other fluids diluted rapidly so that at the end of inflation the Universe is cold and almost empty of particles. Therefore, to recover the hot standard big bang, a reheating mechanism is required [52–62].

In 1995, a different scenario for inflation was proposed [28], which is known as warm inflation. In warm inflation, it is still assumed that the inflaton is still the dominant component and it also varies slowly; however, there are some differences. One of the main differences of warm inflation is that it assumes that there is radiation along with inflaton, so that these two have interaction during the whole time of inflation. Because of the interaction, energy transfers from inflaton to the radiation, and the Universe remains warm at the end of reheating. Then, it comes to the second difference, which is that there is no need for the reheating mechanism in the scenario of warm inflation. The next difference is about the fluctuations. In contrast to cold inflation,[1] where the fluctuations are quantum type [47–50], in warm inflation, we have both quantum and thermal fluctuations, and the thermal fluctuations dominate as long as the condition $T > H$ is satisfied [29,30,63–66].

Inspired by Ref. [67], we are going to consider the role of holographic dark energy (HDE) in the very early Universe. In other words, it is assumed that inflation is derived by HDE, known as a candidate of dark energy that provides interesting results for the late time evolution of the Universe [68–71] (see [72] for a review on HDE). The HDE is given by $\rho = 3c^2M_p^2/L^2$, where c is a dimensionless parameter and the length scale L is known as the infrared cutoff L_{IR}. One of the motivations for studying the HDE for inflation is the possibility of having large HDE due to the small length scale L [67,73–75]. In the present work, we will study the role of HDE in warm inflation; namely, it is assumed that there is also radiation and during inflationary times HDE and radiation interact with each other. The topic has been considered for the scenario of cold inflation; however, we could not find any literature in the frame of warm inflation.

There are different choices for the length scale L, such as different horizons and the Ricci scalar. It has been shown that the Hubble horizon for the HDE could not

*a.mohammadi@uok.ac.ir; abolhassanm@gmail.com

[1]The standard inflationary scenario assumes that the scalar field is the dominant component that drives inflation. All other fluids diluted rapidly, and the Universe is cold at the end of inflation. This is why it is also known as "cold inflation."

provide desirable results, and it could not provide a suitable description for the present accelerating Universe [76]. Reference [77] reconsidered the HDE with the Hubble length including a varying parameter c. The results were promising in which the model could properly describe the late time acceleration. It motivates us to consider the same model of dark energy density in the scenario of warm inflation. Then, the length scale is taken as the Hubble horizon, and the parameter c will be assumed to vary instead of being constant. Moreover, the model will be studied for the strong dissipation regime of warm inflation. One of the main reasons for this choice is that the scenario of warm inflation in the strong dissipation regime has the ability to come to an agreement with the swampland criteria [78–80], which recently have got cosmologists' attention as a measure to classify inflationary models [81–93].

The paper has been organized as follows: In Sec. II, the scenario of warm inflation briefly is reviewed. In Sec. III, the HDE is taken as the source of inflation, and the main dynamical equations are derived. Then, we derive the perturbation parameters and, by comparing the results with data, the free constants are determined. Next, we consider the energy scale of inflation and also investigate the validity of the main assumptions of the model. Finally, the results will be summarized in Sec. IV.

II. BRIEF REVIEW ON WARM INFLATION

The main dynamical equations are two Friedmann equations:

$$H^2 = \frac{1}{3M_p^2}(\rho_{\rm inf} + \rho_r), \tag{1}$$

$$\dot{H} = \frac{-1}{2M_p^2}((\rho_{\rm inf} + p_{\rm inf}) + (\rho_r + p_r)), \tag{2}$$

and the evolution equations of the fluids as [94]

$$\dot{\rho}_{\rm inf} + 3H(\rho_{\rm inf} + p_{\rm inf}) = -\Gamma(\rho_{\rm inf} + p_{\rm inf}), \tag{3}$$

$$\dot{\rho}_r + 3H(\rho_r + p_r) = \Gamma(\rho_{\rm inf} + p_{\rm inf}), \tag{4}$$

where the subscript "inf" stands for the fluid that drives inflation (e.g., it is $\rho_{\rm inf} = \rho_\phi$ when the scalar field is the source of inflation) and the subscript "r" stands for radiation. Also, the quantity Γ is known as the dissipation coefficient, which could be constant, depends on temperature T_r or scalar field, or depends on both temperature and scalar field.

The same as cold inflation, we have slow-roll approximations which are usually described by the slow-roll parameters. The first slow-roll parameter is defined as

$$\epsilon_1 = \frac{-\dot{H}}{H^2}, \tag{5}$$

and the next slow-roll parameters are defined through a hierarchy relation as follows:

$$\epsilon_{n+1} = \frac{\dot{\epsilon}_n}{H\epsilon_n}. \tag{6}$$

Also, there is another type of the slow-roll parameter in warm inflation, which is given by

$$\beta = \frac{\dot{\Gamma}}{H\Gamma}. \tag{7}$$

This parameter describes the evolution of the dissipation coefficient during inflationary time. The dissipation coefficient that we are going to consider is given by

$$\Gamma = C\frac{T^m}{\phi^{m-1}}, \tag{8}$$

where ϕ is the scalar field that drives inflation. This dissipation coefficient has been considered in many models of warm inflation [66,90,95–98], where the cases $m = 3, 1, -1$ are the ones that have received the most interest.

There are both quantum and thermal fluctuations in the scenario of warm inflation, and the thermal fluctuations dominate as long as $T > H$ [29,30,63–66,95,96]. The amplitude of the scalar perturbations is given by [66,90,95,96]

$$\mathcal{P}_s = \frac{H^2}{8\pi^2 M_p^2 \epsilon_1}\left[1 + 2n_{\rm BE} + \frac{2\sqrt{3}\pi Q}{\sqrt{3+4\pi Q}}\frac{T}{H}\right]G(Q), \tag{9}$$

where $n_{\rm BE}$ is the Bose-Einstein distribution given by $n_{\rm BE} = (\exp(H/T_{\rm inf}) - 1)^{-1}$, where $T_{\rm inf}$ is the inflaton fluctuation which is not required to necessarily be equal to radiation temperature T_r. Also, $G(Q)$ is a function of the dissipative ratio Q, defined as $Q \equiv \Gamma/3H$, which is the result of coupling between inflaton fluctuations and radiation. The exact form of $G(Q)$ depends on the dissipation coefficient, and it is determined by solving the set of perturbation equations. For the dissipation coefficient (8), the function $G(Q)$ could be found numerically which is given by [66,90,95,96]

$$G(Q) = 1 + 4.981Q^{1.946} + 0.127Q^{4.330} \quad \text{for } m = 3, \tag{10}$$

$$G(Q) = 1 + 0.335Q^{1.364} + 0.0185Q^{2.315} \quad \text{for } m = 1, \tag{11}$$

and

$$G(Q) = \frac{1 + 0.4Q^{0.77}}{(1 + 0.15Q^{1.09})^2} \quad \text{for } m = -1. \tag{12}$$

For the strong dissipative regime, which we are interested in, the dissipative parameter Q is bigger than one, i.e., $Q \gg 1$. Then, the function, in general, could be written as $G(Q) = a_m Q^{b_m}$, where the constants a_m and b_m depend on the value of the constant m.

The scalar spectral index is defined through the amplitude of the scalar perturbation as

$$n_s - 1 = \frac{d\ln(\mathcal{P}_s)}{d\ln(k)}. \tag{13}$$

The observational data determine that the scalar spectral index should be $n_s = 0.9642 \pm 0.0042$, according to Planck-2018 data [42], which is very close to one. Note that $n_s = 1$ corresponds to scale-invariant fluctuations (see [49–51] for more detail).

The amplitude of the tensor perturbation is read as [95,96]

$$\mathcal{P}_t = \frac{2H^2}{\pi^2 M_p^2}. \tag{14}$$

The next perturbation parameter, which is widely used to test the inflationary model, is the tensor-to-scalar ratio r, defined by

$$r = \frac{\mathcal{P}_t}{\mathcal{P}_s}. \tag{15}$$

There are still no exact data for the parameter, and the latest observational data indicate only an upper limit for the parameter as $r < 0.064$ [42].

The amount of expansion of the Universe during inflation is measured through the parameter N, known as the number of e-folds, which is defined by

$$N = \int_{t_\star}^{t_e} H dt, \tag{16}$$

in which the subscripts e and $\star$, respectively, indicate the end of inflation and the time of horizon crossing. Using this relation, one could relate a parameter at the initial time to its value at the end of inflation.

III. HDE FOR WARM INFLATION

In this section, it is assumed that HDE is the source of inflation, i.e., $\rho_{\rm inf} = \rho_{\rm HDE}$. The HDE is given by

$$\rho_{\rm HDE} = \frac{3c^2 M_p^2}{L^2}, \tag{17}$$

where L is the infrared cutoff and c is a dimensionless parameter which usually is taken as a constant; however, it could vary in a general case.

Here, the infrared cutoff is taken as the Hubble length, i.e., $L = H^{-1}$, and the parameter c is assumed to vary instead of being constant. Such a case of HDE is studied for the late time behavior of the Universe in Ref. [77], which led to interesting results. On the other hand, it is assumed that, since inflation occurs in a high-energy regime, there is an ultraviolet correction to the infrared cutoff. The presence of such corrections is also assumed to be included in the parameter c. Then, for the Friedmann equation, we have

$$H^2 = \frac{1}{3M_p^2}(3c^2 M_p^2 H^2 + \rho_r). \tag{18}$$

From the radiation conservation equation [Eq. (4)] and by imposing the quasistable production of the radiation, i.e., $\dot{\rho} \ll H\rho_r, \Gamma(\rho_{\rm inf} + p_{\rm inf})$, one arrives at

$$4H\rho_r = \Gamma(\rho_{\rm HDE} + p_{\rm HDE}). \tag{19}$$

By using the second Friedmann equation [Eq. (2)], the radiation energy density is read as

$$\rho_r = \frac{-3M_p^2}{2}\frac{Q}{1+Q}\dot{H}; \tag{20}$$

note that, since energy density is positive, the time derivative of the Hubble parameter should be negative. The quantity Q is known as the dissipative parameter defined as $Q \equiv \Gamma/3H$.

Substituting Eq. (20) in the Friedmann equation [Eq. (18)], the time derivative of the Hubble parameter is obtained as

$$\dot{H} = -2(1-c^2)\frac{1+Q}{Q}H^2. \tag{21}$$

Inserting the result in Eq. (20), the radiation energy density is rewritten in terms of the parameter c and the Hubble parameter as

$$\rho_r = 3M_p^2(1-c^2)H^2. \tag{22}$$

On the other hand, the radiation energy density is expressed in terms of its temperature

$$\rho_r = \sigma T_r^4, \tag{23}$$

where σ is the Stephen-Boltzmann constant given by $\sigma = \pi^2 g_\star/30$, where $g_\star$ is the number of degrees of freedom of the radiation field. T_r is the temperature of the radiation. Comparing Eqs. (22) and (23), the temperature is obtained as follows:

$$T_r^4 = \frac{3M_p^2}{\sigma}(1-c^2)H^2. \tag{24}$$

From the definition of ϵ_1 and using Eq. (21), the parameter, in general, is read as

$$\epsilon_1 = 2(1-c^2)\frac{1+Q}{Q}. \tag{25}$$

The second slow-roll parameter is obtained from Eq. (6) as

$$\epsilon_2 = \eta - \frac{1}{1+Q}(\beta - \epsilon_1), \tag{26}$$

where the new parameter η is defined as

$$\eta = \frac{-2c\dot{c}}{H(1-c^2)}. \tag{27}$$

The introduced dissipation coefficient depends on both the temperature and the scalar field ϕ, which plays the role of inflaton. To go for more detail, the dependence of the scalar field should be specified. Here, the HDE drives inflation, and it could be said that it plays the role of inflaton ϕ. Also, there are works of literature where the correspondence between the HDE and the scalar field has been studied [99–104]. Therefore, it is assumed that the HDE could be related to a type of scalar field which depends on the temperature as $\phi \propto T^{\lambda}$. Then, substituting it in Eq. (8), the dissipation coefficient is rewritten as $\Gamma = C_T T^p$, where C_T and λ are two constants and the parameter p is defined as $p = m - \lambda(m-1)$. Then, using Eq. (24), it is expressed in terms of the parameter c and the Hubble parameter:

$$\Gamma = C_T \left(\frac{3M_p^2}{\sigma}(1-c^2)H^2\right)^{p/4}. \tag{28}$$

The result could be utilized in Eq. (7), so that the slow-roll parameter β is simplified as

$$\beta = -2(1-c^2)\frac{1+Q}{Q}\frac{H\Gamma_{,H}}{\Gamma}. \tag{29}$$

A. Holographic warm inflation in HDR

For the rest of the work, it is assumed that inflation occurs in the high dissipative regime (HDR), i.e., $Q \gg 1$. Imposing this condition on the equations, and by substituting the radiation energy density (20) in Eq. (18), the first slow-roll parameter is obtained only in terms of the parameter c as

$$\epsilon_1 = \frac{-\dot{H}}{H^2} = 2(1-c^2). \tag{30}$$

Then, utilizing the hierarchy definition of the slow-roll parameters, the second one is given by

$$\epsilon_2 = \frac{\dot{\epsilon_1}}{H\epsilon_1} = \frac{-2c\dot{c}}{H(1-c^2)}. \tag{31}$$

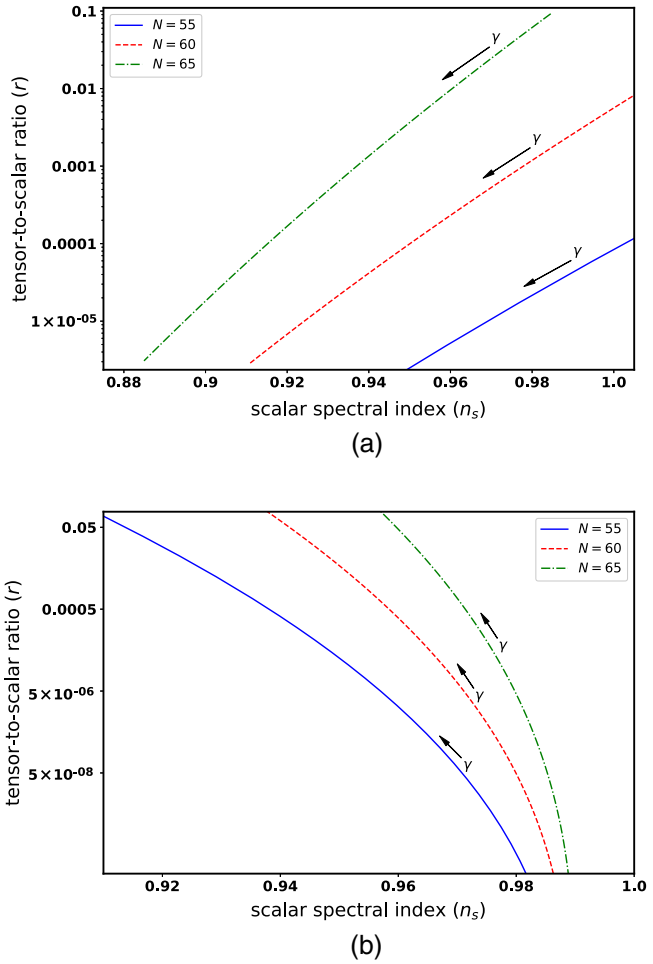

FIG. 1. The figure illustrates the tensor-to-scalar ratio r versus the scalar spectral index n_s for different values of the number of e-folds. Here, γ is taken as the variable, and the arrow for each curve shows the direction of increasing γ. The figure shows the values of n_s and r at the time of the horizon crossing. The other constants are taken as (a) $m = 3$, $\lambda = 2$, and $c_0 = 0.57$ and (b) $m = -1$, $\lambda = -1$, and $c_0 = 0.51$.

The parameter c is assumed to be given by $c = c_0 H^{\gamma}$, where c_0 and γ are constants[2] which will be determined later in a comparison with observational data. By this definition, we have

$$\dot{H} = -2(1 - c_0^2 H^{2\gamma})H^2. \tag{32}$$

Inserting the above relation in the equation of number of e-folds (16), we have

[2]In a general case for the HDE, the parameter c is considered to be a slowly varying function instead of being constant. On the other hand, during the slow-roll inflationary phase, the Hubble parameter is taken as a slowly varying function, which is described by the smallness of the parameter ϵ_1. Therefore, the parameter c is taken to be proportional to the Hubble parameter to satisfy slowly varying behavior.

TABLE I. The table shows numerical results for the scalar spectral index and the tensor-to-scalar ratio for different values of the number of e-folds N and γ. The other constants are taken as $m = 3$, $\lambda = 2$, and $c_0 = 0.57$.

N	γ	n_s	r
55	0.0205	0.9662	8.15×10^{-6}
55	0.0192	1.0176	2.67×10^{-4}
55	0.0180	1.0766	9.89×10^{-3}
60	0.0205	0.9239	9.74×10^{-6}
60	0.0192	0.9646	3.39×10^{-4}
60	0.0180	1.0117	0.0135
65	0.0205	0.8956	1.09×10^{-5}
65	0.0192	0.9282	4.00×10^{-4}
65	0.0180	0.9659	0.0169

TABLE II. The table shows numerical results for the scalar spectral index and the tensor-to-scalar ratio for different values of the number of e-folds N and γ. The other constants are taken as $m = -1$, $\lambda = -1$, and $c_0 = 0.52$.

N	γ	n_s	r
55	0.025	0.9625	9.43×10^{-7}
55	0.023	0.9462	7.97×10^{-5}
55	0.021	0.9207	0.0148
60	0.025	0.9746	1.00×10^{-6}
60	0.023	0.9637	8.82×10^{-5}
60	0.021	0.9458	0.0173
65	0.025	0.9819	1.04×10^{-6}
65	0.023	0.9747	9.40×10^{-5}
65	0.021	9.623	0.0193

$$N = -\int_{H_\star}^{H_e} \frac{1}{2(1 - c_0^2 H^{2\gamma})H} dH.$$

The parameter H_e is found from the relation $\epsilon_1 = 1$, which indicates the end of inflation. By solving the above integral, the Hubble parameter is obtained in terms of the number of e-folds as

$$H^{2\gamma}(N) = \frac{e^{4\gamma N}}{c_0^2(1 + e^{4\gamma N})}. \tag{33}$$

Then, from the definition of c, the parameter is found in terms of N, i.e.,

$$c^2(N) = \frac{e^{4\gamma N}}{1 + e^{4\gamma N}}. \tag{34}$$

Since both the slow-roll parameters were expressed in terms of the parameter c, they could also be rewritten in terms of the number of e-folds, as follows:

$$\epsilon_1(N) = \frac{2}{1 + e^{4\gamma N}}, \tag{35}$$

$$\epsilon_2(N) = \frac{4\gamma e^{4\gamma N}}{1 + e^{4\gamma N}}. \tag{36}$$

The next slow-roll parameter is given by

$$\beta(N) = -p\left[1 - (1 + \gamma)\frac{e^{4\gamma N}}{1 + e^{4\gamma N}}\right]. \tag{37}$$

By computing Eq. (13) for the HDR, the scalar spectral index is obtained as

TABLE III. The table shows the numerical results of the model for different values of the constants.

m	p	N	γ	c_0	n_s	r	Energy scale	T/H	ρ_H/ρ_r
3	2	60	0.0192	0.55	0.9645	0.0140	9.74×10^{15}	37.82	100.283
3	2	60	0.0192	0.57	0.9645	3.39×10^{-4}	3.84×10^{15}	95.892	100.283
3	2	65	0.0192	0.55	0.9282	0.0165	1.01×10^{16}	33.009	147.230
3	2	65	0.0192	0.57	0.9282	4.00×10^{-4}	4.01×10^{15}	83.676	147.230
3	2	60	0.0180	0.57	1.0117	0.0135	9.65×10^{15}	40.968	75.188
3	2	60	0.0180	0.59	1.0117	2.93×10^{-4}	3.70×10^{15}	106.779	75.188
3	2	65	0.0180	0.57	0.9659	0.0169	1.02×10^{16}	35.466	107.770
3	2	65	0.0180	0.59	0.9659	3.66×10^{-4}	3.91×10^{15}	92.438	107.770
−1	−1	60	0.0231	0.49	0.9643	0.0119	9.36×10^{15}	31.243	255.698
−1	−1	60	0.0231	0.51	0.9643	3.72×10^{-4}	3.93×10^{15}	74.272	255.698
−1	−1	65	0.0231	0.49	0.9752	0.0126	9.51×10^{15}	27.414	405.856
−1	−1	65	0.0231	0.51	0.9752	3.96×10^{-4}	4.00×10^{15}	65.169	405.856
−1	−1	60	0.0215	0.51	0.9511	0.0258	1.13×10^{16}	28.303	174.164
−1	−1	60	0.0215	0.53	0.9511	7.22×10^{-4}	4.64×10^{15}	69.238	174.164
−1	−1	65	0.0215	0.51	0.9661	0.0283	1.16×10^{16}	24.847	267.73
−1	−1	65	0.0215	0.53	0.9661	7.92×10^{-4}	5.75×10^{15}	60.784	267.73

$$ns - 1 = (b_m - 0.5)\epsilon_1 - \epsilon_2 + \left(b_m + \frac{1}{m} + 0.5\right)\beta, \quad (38)$$

and the tensor-to-scalar ratio is acquired from Eqs. (9) and (14) as follows:

$$r = 16\epsilon_1 \left(\sqrt{3\pi}\frac{T}{H} a_m Q^{b_m}\right)^{-1}. \quad (39)$$

In the subsequent subsection, the parameters are estimated, and the results of the model will be compared with data.

B. Comparing the model with data

To verify the validity of the model, its results should be compared with observational data, or one could apply the observational data and constrain the free constants of the model. In this regard, first, we need to express the perturbation parameters $\mathcal{P}_s$, n_s, and r in terms of the number of e-folds. This way, the parameters could be easily estimated at the time of the horizon crossing. Following Refs. [67,73–75], it is assumed that Eqs. (38) and (39) provide acceptable approximate values for the inflationary observable parameters.

Using Eqs. (35) and (37), the scalar spectral index is expressed in terms of the number of e-folds. Next, through Eqs. (9), (24), (28), and (33), it is achieved that

$$\left(\sqrt{3\pi}\frac{T}{H} a_m Q^{b_m}\right)\Big|_\star = \frac{8\pi^2 M_p^2 \mathcal{P}_s^\star \epsilon_1(N)}{H^2(N)}. \quad (40)$$

Then, substituting Eq. (40) in Eq. (39), the tensor-to-scalar ratio also is read in terms of the number of e-folds. Figure 1 illustrates the tensor-to-scalar ratio r versus the scalar spectral index n_s at the time of horizon crossing. The figure shows the $r - n_s$ diagram for two values of m, in Eq. (8), as $m = 3$ and $m = -1$. Note that, for $m = 1$, there is no consistency with the results and observational data. The curves are plotted for different values of the number of e-folds which are mostly used in the literature. The latest data state that $n_s = 0.9642 \pm 0.0049$ and $r \leq 0.064$. By increasing the number of e-folds, the curves go out of the observational region. However, for a smaller number of e-folds, the tensor-to-scalar ratio r gets smaller values. The varying parameters of the curves are the parameter γ, in which, for $m = 3$, increasing of the parameter γ leads to the reduction of both the scalar spectral index and tensor-to-scalar ratio. The situation is different for $m = -1$ so that, by enhancement of the parameter γ, the scalar spectral index increases; however, the tensor-to-scalar parameter decreases. Moreover, by taking smaller N, the curve stays in the observational range for bigger values of γ. Tables I and II determine the numerical results for both cases of $m = 3$ and $m = -1$, where the above conclusions are restated by numbers to give more insight. More results are presented in Table III, where the energy scale of inflation is estimated and the conditions of the model, which is discussed in the next subsection, are investigated.

Figure 2 exhibits the same plot for different values of the constant c_0. The constant c_0 appears in the tensor-to-scalar ratio. The figure displays that, by enhancement of c_0, r dramatically decreases.

By comparing the model with observational data, we are provided with a general view of the values of the constants of the model to have an agreement with observation. Taking these values of the constants, we could have a general insight about the energy density ρ_H, which displays the energy scale of inflation. Figure 3 portrays the behavior of the HDE during the inflationary time. It is concluded that the inflation starts at the energy scale of about 10^{15} GeV, which decreases by approaching the end of inflation.

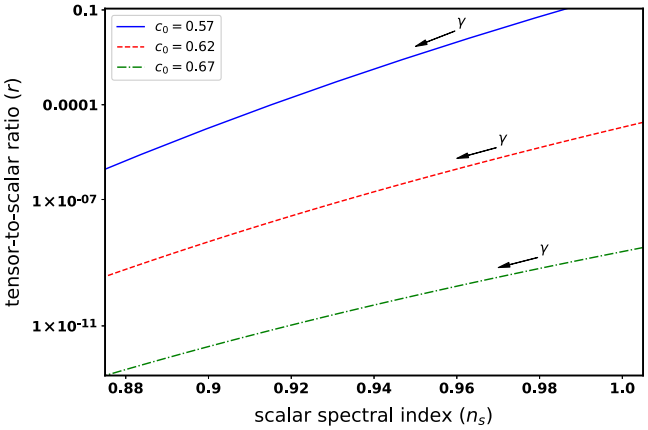

(a)

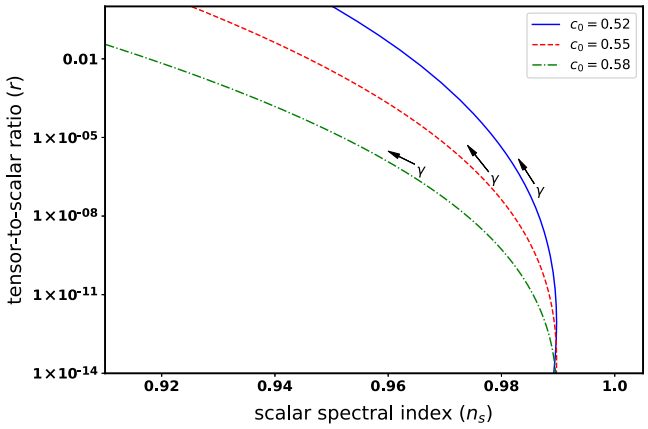

(b)

FIG. 2. The plot is a parametric plot displaying the tensor-to-scalar ratio r versus the scalar spectral index n_s for different values of c_0. The same as Fig. 1, the variable is γ. It is realized that by decreasing of the c_0 the curves goes out of the observational range; however, by enhancement of c_0, it comes inside and the parameter r becomes very small. The number of e-folds is taken as $N = 65$, and the other constants are taken as (a) $m = 3$ and $\lambda = 2$ and (b) $m = -1$ and $\lambda = -1$.

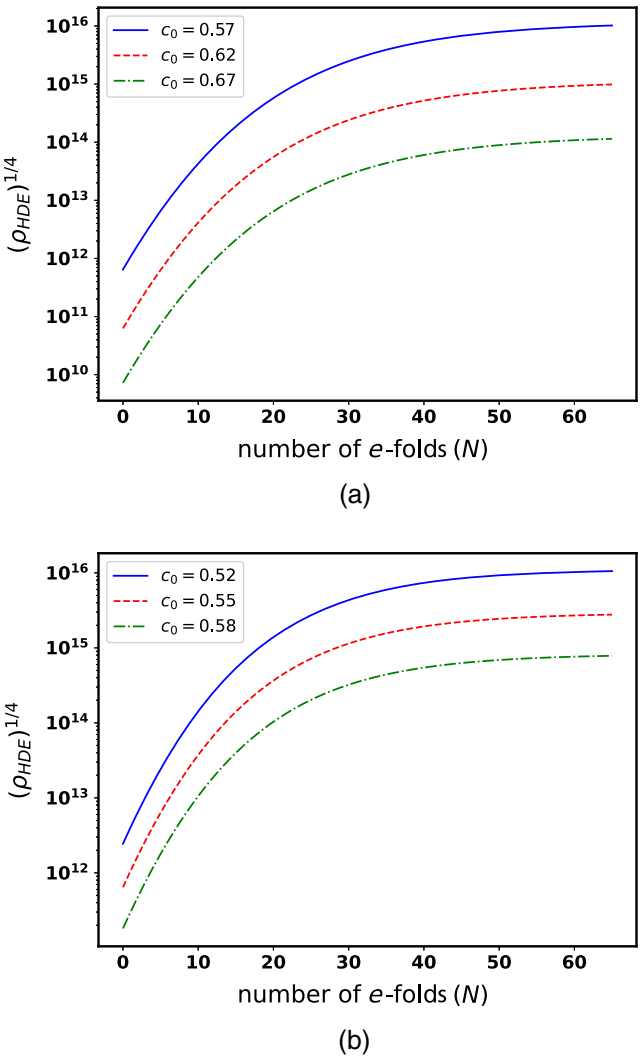

FIG. 3. The behavior of the HDE during the inflationary times is presented for different values of c_0. It has a high value at the initial time, and then it decreases by passing the time. It is seen that the energy scale of inflation is about 10^{15} GeV. The plot also indicates that HDE has smaller values for bigger values of γ. The other constants are taken as (a) $\gamma = 0.018$, $m = 3$, $\lambda = 2$, and $c_0 = 0.57$ and (b) $\gamma = 0.021$, $m = -1$, $\lambda = -1$, and $c_0 = 0.52$.

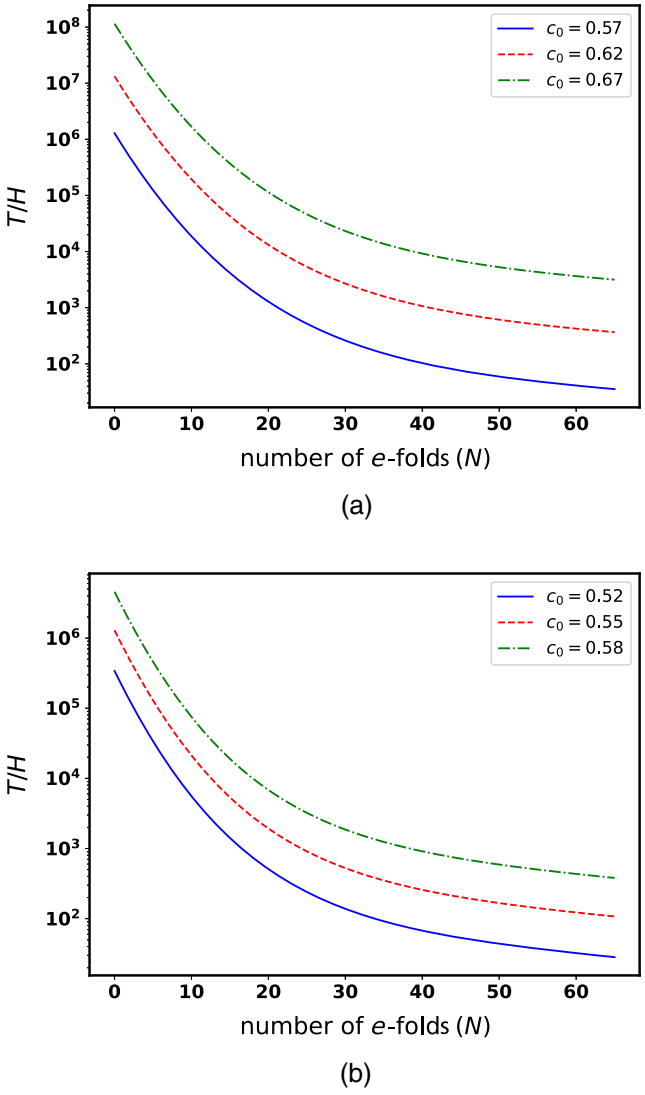

FIG. 4. The term T/H is plotted versus the number of e-folds for different values of the constant γ. The curves shows the value of the term during the inflationary time. It is seen that the condition $T/H > 1$ is verified for the whole time of inflation. The other constants are taken as (a) $\gamma = 0.018$, $m = 3$, and $\lambda = 2$ and (b) $\gamma = 0.021$, $m = -1$, and $\lambda = -1$.

Note that the number of e-folds $N = 0$ indicates the end of inflation, and higher values of number of e-folds means we go more and more inside inflation. In other words, over time and approaching the end of inflation, the number of e-folds decreases. Therefore, in Fig. 3 and also the subsequent figures, the direction of time is actually from right to left.

C. Verifying the conditions of the model

In the scenario of warm inflation, we have two fundamental assumptions as $T/H > 1$ and $\rho_{\rm HDE}/\rho_r > 1$. These assumptions should be verified for the obtained values of the constants. Figure 4 displays the term T/H versus the number of e-folds for different values of c_0 for both $m = 3$ and $m = -1$. It is verified that the term is greater than one, and the condition $T/H > 1$ is verified. Also, the term increases by approaching the end of inflation.

A comparison of the energy densities is presented in Fig. 5. The plot exhibits the ratio $\rho_{\rm HDE}/\rho_r$ for different values of c_0 during inflation, for both cases of m as $m = 3$ and $m = -1$. It is realized that, at the initial times, the HDE is much bigger than the radiation energy density. Then, the HDE is the dominant component, and the assumption that the warm inflation is driven by HDE is verified. By passing time, they come close together so that at the end of inflation they are comparable to each other. Note that, at the

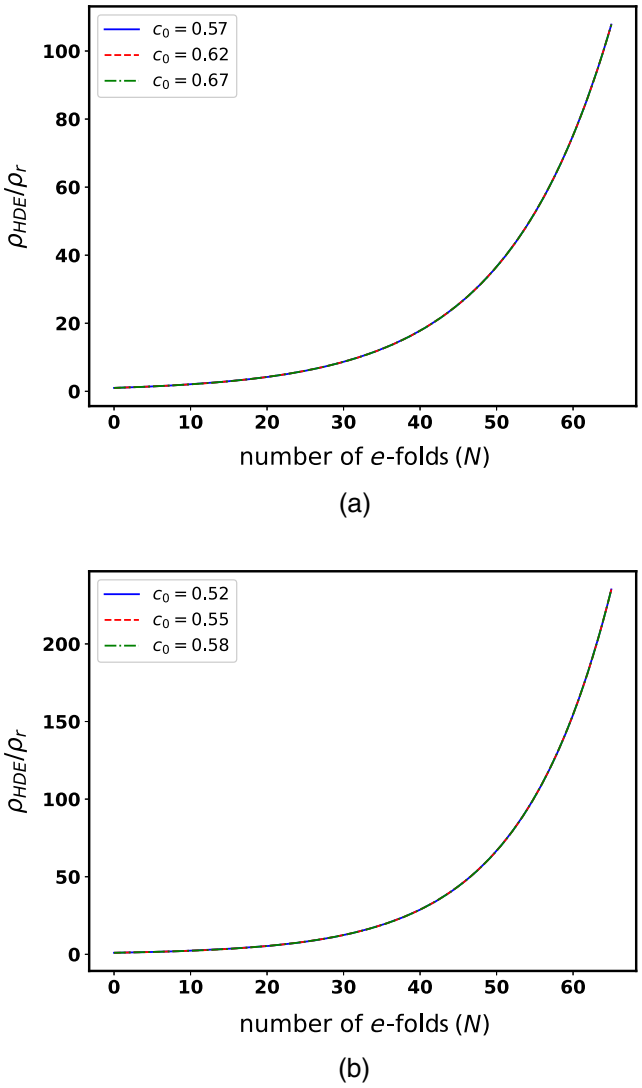

FIG. 5. The plot illustrates the ratio of energy densities of the HDE and radiation during the inflationary times. At the initial time HDE is much bigger, and, by passing the time and approaching the end of inflation, they come close together. The other constants are taken as (a) $\gamma = 0.018$, $m = 3$, $\lambda = 2$, and $c_0 = 0.57$ and (b) $\gamma = 0.021$, $m = -1$, $\lambda = -1$, and $c_0 = 0.52$.

resolution scale of the figures, the difference of the curves $\rho_{\mathrm{HDE}}/\rho_r$ is not distinguishable.

IV. CONCLUSION

The scenario of warm inflation was considered by this assumption that the HDE is the source of inflation. Based on the assumptions of the scenario of warm inflation, we now have two components as HDE and radiation. They interact with each other, and the energy transfers from HDE to the radiation. Moreover, the scenario predicts two types of fluctuations as quantum and thermal fluctuation, respectively, are proportional to H and T. The thermal fluctuations dominate over the quantum fluctuation as long as the condition $T/H > 1$ is preserved.

The infrared of the HDE was assumed to be given by the Hubble length, and we also included this assumption that the parameter c, which appears in the HDE, is a varying parameter instead of being constant. Then, the dynamical equations of the model and also the main perturbations parameter were derived. The inflation was assumed to occur at the strong dissipative regime, and the dissipation coefficient Γ was taken to depend on the temperature T. Next, the perturbation parameters were estimated at the time of the horizon crossing, and, by comparing them with observational data, we could determine the free constants of the model. This was performed for different types of temperature dependence of the dissipation coefficient. The $r - n_s$ diagram of the model was depicted, and it was realized that the model could come to a good agreement with data. Next, the behavior of the HDE was investigated. The HDE was assumed for the source of inflation; i.e., it is the dominant component. Therefore, its energy density at the initial times gives the energy scale of inflation. The behavior of HDE was plotted, which displayed that the energy scale of inflation is around 10^{15} GeV.

At the final step, we reconsider the verification of the fundamental conditions of the model, i.e., $T/H > 1$ and $\rho_{\mathrm{HDE}}/\rho_r \gg 1$, for the determined values of the constants. The first condition guarantees that the thermal fluctuations dominate over the quantum fluctuations. The behavior of the term T/H was plotted in Fig. 4. It shows that the term is greater than one for the whole time of inflation. Also, it gets larger over time. The ratio $\rho_{\mathrm{HDE}}/\rho_r \gg 1$ was illustrated in Fig. 5, which determines that, at the initial time, the HDE is much bigger than one. This result verifies the assumption that inflation is driven by the HDE. By approaching the end of inflation, the ratio gets smaller, stating that the two densities come closer. A numerical result of the model is presented in Table III.

ACKNOWLEDGMENTS

The work of A. M. has been supported financially by Vice Chancellorship of Research and Technology, University of Kurdistan under research Project No. 99/11/19063. He also thanks the referee for his/her comments, which improved the quality of the manuscript.

[1] A. A. Starobinsky, A new type of isotropic cosmological models without singularity, Phys. Lett. **91B**, 99 (1980).
[2] A. H. Guth, The inflationary Universe: A possible solution to the horizon and flatness problems, Phys. Rev. D **23**, 347 (1981).
[3] A. Albrecht and P. J. Steinhardt, Cosmology for Grand Unified Theories with Radiatively Induced Symmetry Breaking, Phys. Rev. Lett. **48**, 1220 (1982).
[4] A. D. Linde, A new inflationary Universe scenario: A possible solution of the horizon, flatness, homogeneity, isotropy and primordial monopole problems, Phys. Lett. **108B**, 389 (1982).
[5] A. D. Linde, Chaotic inflation, Phys. Lett. **129B**, 177 (1983).
[6] G. Barenboim and W. H. Kinney, Slow roll in simple non-canonical inflation, J. Cosmol. Astropart. Phys. 03 (2007) 014.
[7] P. Franche, R. Gwyn, B. Underwood, and A. Wissanji, Initial conditions for non-canonical inflation, Phys. Rev. D **82**, 063528 (2010).
[8] S. Unnikrishnan, V. Sahni, and A. Toporensky, Refining inflation using non-canonical scalars, J. Cosmol. Astropart. Phys. 08 (2012) 018.
[9] K. Rezazadeh, K. Karami, and P. Karimi, Intermediate inflation from a non-canonical scalar field, J. Cosmol. Astropart. Phys. 09 (2015) 053.
[10] K. Saaidi, A. Mohammadi, and T. Golanbari, Light of Planck-2015 on noncanonical inflation, Adv. High Energy Phys. **2015**, 1 (2015).
[11] M. Fairbairn and M. H. G. Tytgat, Inflation from a tachyon fluid?, Phys. Lett. B **546**, 1 (2002).
[12] S. Mukohyama, Brane cosmology driven by the rolling tachyon, Phys. Rev. D **66**, 024009 (2002).
[13] A. Feinstein, Power law inflation from the rolling tachyon, Phys. Rev. D **66**, 063511 (2002).
[14] T. Padmanabhan, Accelerated expansion of the Universe driven by tachyonic matter, Phys. Rev. D **66**, 021301 (2002).
[15] A. Aghamohammadi, A. Mohammadi, T. Golanbari, and K. Saaidi, Hamilton-Jacobi formalism for tachyon inflation, Phys. Rev. D **90**, 084028 (2014).
[16] M. Spalinski, On power law inflation in DBI models, J. Cosmol. Astropart. Phys. 05 (2007) 017.
[17] D. Bessada, W. H. Kinney, and K. Tzirakis, Inflationary potentials in DBI models, J. Cosmol. Astropart. Phys. 09 (2009) 031.
[18] J. M. Weller, C. van de Bruck, and D. F. Mota, Inflationary predictions in scalar-tensor DBI inflation, J. Cosmol. Astropart. Phys. 06 (2012) 002.
[19] N. Nazavari, A. Mohammadi, Z. Ossoulian, and K. Saaidi, Intermediate inflation driven by DBI scalar field, Phys. Rev. D **93**, 123504 (2016).
[20] K.-i. Maeda and K. Yamamoto, Stability analysis of inflation with an su (2) gauge field, J. Cosmol. Astropart. Phys. 12 (2013) 018.
[21] A. A. Abolhasani, R. Emami, and H. Firouzjahi, Primordial anisotropies in gauged hybrid inflation, J. Cosmol. Astropart. Phys. 05 (2014) 016.
[22] S. Alexander, D. Jyoti, A. Kosowsky, and A. Marcianò, Dynamics of gauge field inflation, J. Cosmol. Astropart. Phys. 05 (2015) 005.
[23] M. Tirandari and K. Saaidi, Anisotropic inflation in Brans–Dicke gravity, Nucl. Phys. **B925**, 403 (2017).
[24] R. Maartens, D. Wands, B. A. Bassett, and I. P. Heard, Chaotic inflation on the brane, Phys. Rev. D **62**, 041301 (2000).
[25] T. Golanbari, A. Mohammadi, and K. Saaidi, Brane inflation driven by noncanonical scalar field, Phys. Rev. D **89**, 103529 (2014).
[26] A. Mohammadi, T. Golanbari, S. Nasri, and K. Saaidi, Brane inflation: Swampland criteria, TCC, and reheating constraint, arXiv:2006.09489.
[27] A. Mohammadi, T. Golanbari, and J. Enayati, Brane inflation and Trans-Planckian censorship conjecture, arXiv:2012.01512.
[28] A. Berera, Warm Inflation, Phys. Rev. Lett. **75**, 3218 (1995).
[29] A. Berera, Warm inflation in the adiabatic regimea model, an existence proof for inflationary dynamics in quantum field theory, Nucl. Phys. **B585**, 666 (2000).
[30] L. M. Hall, I. G. Moss, and A. Berera, Scalar perturbation spectra from warm inflation, Phys. Rev. D **69**, 083525 (2004).
[31] K. Sayar, A. Mohammadi, L. Akhtari, and K. Saaidi, Hamilton-Jacobi formalism to warm inflationary scenario, Phys. Rev. D **95**, 023501 (2017).
[32] L. Akhtari, A. Mohammadi, K. Sayar, and K. Saaidi, Viscous warm inflation: HamiltonJacobi formalism, Astropart. Phys. **90**, 28 (2017).
[33] H. Sheikhahmadi, A. Mohammadi, A. Aghamohammadi, T. Harko, R. Herrera, C. Corda, A. Abebe, and K. Saaidi, Constraining chameleon field driven warm inflation with Planck 2018 data, Eur. Phys. J. C **79**, 1038 (2019).
[34] A. Mohammadi, T. Golanbari, H. Sheikhahmadi, K. Sayar, L. Akhtari, M. Rasheed, and K. Saaidi, Warm tachyon inflation and swampland criteria, Chin. Phys. C **44**, 095101 (2020).
[35] A. Mohammadi, K. Saaidi, and T. Golanbari, Tachyon constant-roll inflation, Phys. Rev. D **97**, 083006 (2018).
[36] A. Mohammadi, K. Saaidi, and H. Sheikhahmadi, Constant-roll approach to non-canonical inflation, Phys. Rev. D **100**, 083520 (2019).
[37] T. Golanbari, A. Mohammadi, and K. Saaidi, Observational constraints on DBI constant-roll inflation, Phys. Dark Universe **27**, 100456 (2020).
[38] A. Mohammadi, T. Golanbari, and K. Saaidi, Beta-function formalism for k-essence constant-roll inflation, Phys. Dark Universe **28**, 100505 (2020).
[39] A. Mohammadi, T. Golanbari, S. Nasri, and K. Saaidi, Constant-roll brane inflation, Phys. Rev. D **101**, 123537 (2020).
[40] P. A. R. Ade *et al.* (Planck Collaboration), Planck 2013 results. XXII. Constraints on inflation, Astron. Astrophys. **571**, A22 (2014).
[41] P. A. R. Ade *et al.* (Planck Collaboration), Planck 2015 results. XX. Constraints on inflation, Astron. Astrophys. **594**, A20 (2016).
[42] Y. Akrami *et al.* (Planck Collaboration), Planck 2018 results. X. Constraints on inflation, Astron. Astrophys. **641**, A10 (2020).

[43] A. D. Linde, Inflationary cosmology, Phys. Rep. **333**, 575 (2000).
[44] A. Linde, Particle physics and inflationary cosmology, Contemp. Concepts Phys. **5**, 362 (1990).
[45] A. D. Linde, Current understanding of inflation, New Astron. Rev. **49**, 35 (2005).
[46] A. D. Linde, Prospects of inflation, Phys. Scr. T **117**, 40 (2005).
[47] A. Riotto, Inflation and the theory of cosmological perturbations, ICTP Lect. Notes Ser. **14**, 317 (2003).
[48] D. Baumann, TASI lecture on inflation, in *Physics of the large and the small, TASI 09, Proceedings of the Theoretical Advanced Study Institute in Elementary Particle Physics, Boulder, Colorado, 2009* (2011), pp. 523–686 [arXiv:0907.5424].
[49] S. Weinberg, *Cosmology* (Oxford University Press, Oxford, 2008).
[50] D. H. Lyth and A. R. Liddle, *The Primordial Density Perturbation: Cosmology, Inflation and the Origin of Structure* (Cambridge University Press, Cambridge, 2009).
[51] A. R. Liddle and D. H. Lyth, *Cosmological Inflation and Large Scale Structure* (Cambridge University Press, Cambridge, 2000).
[52] L. F. Abbott, E. Farhi, and M. B. Wise, Particle production in the new inflationary cosmology, Phys. Lett. **117B**, 29 (1982).
[53] A. Albrecht, P. J. Steinhardt, M. S. Turner, and F. Wilczek, Reheating an Inflationary Universe, Phys. Rev. Lett. **48**, 1437 (1982).
[54] A. D. Dolgov and A. D. Linde, Baryon asymmetry in inflationary Universe, Phys. Lett. **116B**, 329 (1982).
[55] A. D. Dolgov and D. P. Kirilova, On particle creation by a time dependent scalar field, Joint Institute for Nuclear Research (1989), https://inis.iaea.org/search/search.aspx?orig_q=RN:21072913.
[56] J. H. Traschen and R. H. Brandenberger, Particle production during out-of-equilibrium phase transitions, Phys. Rev. D **42**, 2491 (1990).
[57] Y. Shtanov, J. H. Traschen, and R. H. Brandenberger, Universe reheating after inflation, Phys. Rev. D **51**, 5438 (1995).
[58] L. Kofman, A. D. Linde, and A. A. Starobinsky, Reheating After Inflation, Phys. Rev. Lett. **73**, 3195 (1994).
[59] L. Kofman, A. D. Linde, and A. A. Starobinsky, Towards the theory of reheating after inflation, Phys. Rev. D **56**, 3258 (1997).
[60] B. A. Bassett, S. Tsujikawa, and D. Wands, Inflation dynamics and reheating, Rev. Mod. Phys. **78**, 537 (2006).
[61] R. Allahverdi, R. Brandenberger, F.-Y. Cyr-Racine, and A. Mazumdar, Reheating in inflationary cosmology: Theory and applications, Annu. Rev. Nucl. Part. Sci. **60**, 27 (2010).
[62] M. A. Amin, M. P. Hertzberg, D. I. Kaiser, and J. Karouby, Nonperturbative dynamics of reheating after inflation: A review, Int. J. Mod. Phys. D **24**, 1530003 (2015).
[63] I. G. Moss and C. Xiong, Non-gaussianity in fluctuations from warm inflation, J. Cosmol. Astropart. Phys. 04 (2007) 007.
[64] C. Graham and I. G. Moss, Density fluctuations from warm inflation, J. Cosmol. Astropart. Phys. 07 (2009) 013.
[65] R. O. Ramos and L. da Silva, Power spectrum for inflation models with quantum and thermal noises, J. Cosmol. Astropart. Phys. 03 (2013) 032.
[66] M. Bastero-Gil, A. Berera, and R. O. Ramos, Shear viscous effects on the primordial power spectrum from warm inflation, J. Cosmol. Astropart. Phys. 07 (2011) 030.
[67] S. Nojiri, S. D. Odintsov, and E. N. Saridakis, Holographic inflation, Phys. Lett. B **797**, 134829 (2019).
[68] S. Nojiri, S. D. Odintsov, and E. N. Saridakis, Modified cosmology from extended entropy with varying exponent, Eur. Phys. J. C **79**, 242 (2019).
[69] S. Nojiri, S. D. Odintsov, E. N. Saridakis, and R. Myrzakulov, Correspondence of cosmology from non-extensive thermodynamics with fluids of generalized equation of state, Nucl. Phys. **B950**, 114850 (2020).
[70] S. Nojiri and S. D. Odintsov, Unifying phantom inflation with late-time acceleration: Scalar phantom-non-phantom transition model and generalized holographic dark energy, Gen. Relativ. Gravit. **38**, 1285 (2006).
[71] S. Nojiri, S. Odintsov, V. Oikonomou, and T. Paul, Unifying holographic inflation with holographic dark energy: A covariant approach, Phys. Rev. D **102**, 023540 (2020).
[72] M. Li, A model of holographic dark energy, Phys. Lett. B **603**, 1 (2004).
[73] A. Oliveros and M. A. Acero, Inflation driven by a holographic energy density, Europhys. Lett. **128**, 59001 (2019).
[74] G. Chakraborty and S. Chattopadhyay, Modified holographic energy density-driven inflation and some cosmological outcomes, Int. J. Geom. Methods Mod. Phys. **17**, 2050066 (2020).
[75] A. Mohammadi, T. Golanbari, K. Bamba, and I. P. Lobo, Tsallis holographic dark energy for inflation, Phys. Rev. D **103**, 083505 (2021).
[76] S. D. H. Hsu, Entropy bounds and dark energy, Phys. Lett. B **594**, 13 (2004).
[77] M. Malekjani, M. Rezaei, and I. A. Akhlaghi, Can holographic dark energy models fit the observational data?, Phys. Rev. D **98**, 063533 (2018).
[78] G. Obied, H. Ooguri, L. Spodyneiko, and C. Vafa, De Sitter space and the swampland, arXiv:1806.08362.
[79] S. K. Garg and C. Krishnan, Bounds on slow roll and the de Sitter swampland, J. High Energy Phys. 11 (2019) 075.
[80] H. Ooguri, E. Palti, G. Shiu, and C. Vafa, Distance and de Sitter conjectures on the swampland, Phys. Lett. B **788**, 180 (2019).
[81] W. H. Kinney, Eternal Inflation and the Refined Swampland Conjecture, Phys. Rev. Lett. **122**, 081302 (2019).
[82] H. Matsui and F. Takahashi, Eternal inflation and swampland conjectures, Phys. Rev. D **99**, 023533 (2019).
[83] C.-M. Lin, Type I hilltop inflation and the refined swampland criteria, Phys. Rev. D **99**, 023519 (2019).
[84] K. Dimopoulos, Steep eternal inflation and the swampland, Phys. Rev. D **98**, 123516 (2018).
[85] W. H. Kinney, S. Vagnozzi, and L. Visinelli, The zoo plot meets the swampland: Mutual (in)consistency of single-field inflation, string conjectures, and cosmological data, Classical Quantum Gravity **36**, 117001 (2019).
[86] H. Geng, A potential mechanism for inflation from swampland conjectures, Phys. Lett. B **805**, 135430 (2020).

[87] S. Das, Warm inflation in the light of swampland criteria, Phys. Rev. D **99**, 063514 (2019).
[88] V. Kamali, M. Motaharfar, and R. O. Ramos, Warm brane inflation with an exponential potential: A consistent realization away from the swampland, Phys. Rev. D **101**, 023535 (2020).
[89] R. Brandenberger, V. Kamali, and R. O. Ramos, Strengthening the de Sitter swampland conjecture in warm inflation, J. High Energy Phys. 08 (2020) 127.
[90] M. Motaharfar, V. Kamali, and R. O. Ramos, Warm inflation as a way out of the swampland, Phys. Rev. D **99**, 063513 (2019).
[91] V. K. Oikonomou, Rescaled Einstein-Hilbert gravity from $f(R)$ gravity: Inflation, dark energy and the swampland criteria, Phys. Rev. D **103**, 124028 (2021).
[92] S. D. Odintsov and V. K. Oikonomou, Swampland implications of GW170817-compatible Einstein-Gauss-Bonnet gravity, Phys. Lett. B **805**, 135437 (2020).
[93] S. D. Odintsov and V. K. Oikonomou, Finite-time singularities in swampland-related dark energy models, Europhys. Lett. **126**, 20002 (2019).
[94] M. Bastero-Gil, A. Berera, and R. O. Ramos, Shear viscous effects on the primordial power spectrum from warm inflation, J. Cosmol. Astropart. Phys. 07 (2011) 030.
[95] M. Bastero-Gil, A. Berera, R. O. Ramos, and J. G. Rosa, Warm Little Inflaton, Phys. Rev. Lett. **117**, 151301 (2016).
[96] A. Berera, J. Mabillard, M. Pieroni, and R. O. Ramos, Identifying universality in warm inflation, J. Cosmol. Astropart. Phys. 07 (2018) 021.
[97] M. Bastero-Gil, A. Berera, I. G. Moss, and R. O. Ramos, Cosmological fluctuations of a random field and radiation fluid, J. Cosmol. Astropart. Phys. 05 (2014) 004.
[98] M. Bastero-Gil, A. Berera, and N. Kronberg, Exploring the parameter space of warm-inflation models, J. Cosmol. Astropart. Phys. 12 (2015) 046.
[99] S. Chattopadhyay, A. Pasqua, and M. Khurshudyan, New holographic reconstruction of scalar field dark energy models in the framework of chameleon Brans-Dicke cosmology, Eur. Phys. J. C **74**, 3080 (2014).
[100] S. Chattopadhyay and A. Pasqua, Consequences of holographic scalar field dark energy models in chameleon brans-dicke cosmology, Springer Proc. Phys. **174**, 487 (2016).
[101] G. C. Samanta, Holographic dark energy (DE) cosmological models with quintessence in bianchi Type-V space time, Int. J. Theor. Phys. **52**, 4389 (2013).
[102] A. Sheykhi, Holographic scalar field models of dark energy, Phys. Rev. D **84**, 107302 (2011).
[103] W.-Q. Yang, Y.-B. Wu, L.-M. Song, Y.-Y. Su, J. Li, D.-D. Zhang, and X.-G. Wang, Reconstruction of new holographic scalar field models of dark energy in Brans-Dicke Universe, Mod. Phys. Lett. A **26**, 191 (2011).
[104] K. Karami and J. Fehri, New holographic scalar field models of dark energy in non-flat Universe, Phys. Lett. B **684**, 61 (2010).